

Contents lists available at [SciVerse ScienceDirect](http://SciVerse.ScienceDirect.com)

Applied Thermal Engineering

journal homepage: www.elsevier.com/locate/apthermeng

A two-dimensional frying model for the investigation and optimisation of continuous industrial frying systems



H. Wu, T.G. Karayiannis*, S.A. Tassou

School of Engineering and Design, Brunel University London, Uxbridge, Middlesex UB8 3PH, United Kingdom

HIGHLIGHTS

- A new two-dimensional model for continuous frying systems was developed.
- Simulation results compared well with industrial plant data.
- The effects of operational factors on final moisture and oil content were systematically analysed.

ARTICLE INFO

Article history:

Received 27 February 2012

Accepted 7 October 2012

Available online 13 October 2012

Keywords:

Frying processes

Transient model

Finite volume method

Control

ABSTRACT

In this study, a coupled two-dimensional transient model was developed to predict the temperature, moisture content and oil uptake as encountered in industrial continuous deep fryers. The set of transient governing equations developed were solved numerically with the variable time-step finite volume method. The mathematical model can be used to analyse the effects of different frying conditions on the moisture, oil and temperature profiles during the frying processes. Numerical results are presented to show the applicability of the developed model and can help researchers and designers to ascertain optimum operational conditions of frying processes. The physical and mathematical construction of the model not only allows extension of the formulae so that the frame of the model can be used in other similar food processes systems, but also utilizes the dynamic characteristics of the fryer for development and evaluation of advanced control strategies.

© 2012 Elsevier Ltd. Open access under [CC BY](http://creativecommons.org/licenses/by/3.0/) license.

1. Introduction

Frying is a widely used and industrially important food process. In addition to the actual production of the desired foodstuff, the designer of the process should consider improving quality, reducing or controlling oil absorption and producing healthier products. Therefore, it is a field of major interest to engineering and scientific researchers, as well as designers, developers and manufacturers [1,2]. Frying is classified as one of the most complex food-processing operations due to the numerous interactions that take place within the food. A generic schematic is depicted in Fig. 1, showing that simultaneous heat and mass transfer occurs during frying. The important parameters in such a process include temperature of oil, frying time, initial moisture content and thickness of slice. Many attempts have been made to combine heat and mass transfer principles to describe the temperature, moisture

content and oil content profiles in a product in deep-fat frying processes. In the literature, numerous research works relating the deep-fat frying modelling are described, which focused on potato chips and French fries [3–11].

A more detailed model of temperature and moisture transport in deep-fat frying of an infinite potato slab was provided by Farkas et al. [12,13]. The separate equations for the two regions, crust and the core, with a moving boundary were considered. However, their model did not include the oil phase. A one-dimensional transport model that includes oil phase to simulate the effects of different frying conditions on the oil, moisture, and temperature profiles during the frying process of tortilla chips was developed by Chen and Moreira [14]. In 1999, a multiphase porous media model was developed and used to predict the moisture migration, oil uptake and energy transport in food material such as a semi-dry potato during deep-fat frying, and were validated with available experimental data by Ni and Datta [15]. Later, a two-dimensional model based on the approach of Ref. [15] was developed for frying and cooling of tortilla chips and a set of coupled heat and mass transfer equations were solved using a 2-D finite element method [16,17].

* Corresponding author. Tel.: +44 (0) 1895 267132; fax: +44 (0) 1895 256392.
E-mail address: tassos.karayiannis@brunel.ac.uk (T.G. Karayiannis).

Nomenclature

a	coefficient [–]
A_{eff}	effective heat transfer area between frying oil and air [m^2]
A_p	specific area [m^2/m^3]
b	source term [–]
c_p	specific heat [$\text{kJ}/\text{kg K}$]
D	oil diffusivity [m^2/s]
E_a	activation energy [kJ/mol]
h_a	natural convective heat transfer coefficient of air [$\text{W}/\text{m}^2 \text{K}$]
h_{fa}	heat transfer coefficient between frying oil and air [$\text{W}/\text{m}^2 \text{K}$]
h_{fg}	latent heat of vaporization [J/kg]
h_{fs}	heat transfer coefficient between frying oil and potato slice surface [$\text{W}/\text{m}^2 \text{K}$]
H_{fo}	oil height inside the fryer [m]
k	thermal conductivity [$\text{W}/\text{m K}$]
L	fryer length up to takeout conveyor [m]
L_{ff}	length of free frying section [m]
\dot{m}	mass flow rate [kg/s]
R_g	universal gas constant [$\text{J}/\text{mol K}$]
S_{VFW}	water vapour source term [$1/\text{s}$]
t	time [s]
T	temperature [K]
v	velocity [m/s]
VF	volume fraction [–]
x	axial coordinate [m]
y	vertical coordinate [m]

Greek letters

δ	potato slice thickness [m]
ρ	density [kg/m^3]
ϕ	generalized variable

Subscripts

a	air
amb	ambient
c	characteristic
eff	effective
E	East
fo	frying oil
FG	foul gas
in	inlet
N	North
ps	potato slice
pss	potato slice surface
P	control volume
rps	raw potato slice
ss	steady state
surf	surface
sw	surface water of raw potato slice
S	South
v	vapour
w	water
W	West
0	initial
1	fuel
2	combustion air
3	foul gas
4	re-circulated exhaust gas
5	combustion products
6	Exhaust gas
7	oil inlet
8	oil outlet
9	air flow
10	raw potato slices
11	surface water of raw potato slices
12	oil return
13	finer removal
14	potato crisp

Bouchon and Pyle [18,19] presented a good review of oil absorption modelling in 2005 and they developed a predictive mechanistic model that can be used to understand the principles behind post-frying cooling oil absorption kinetics, which is helpful to identify the parameters such as pressure that affect the final oil intake by the fried product. Halder et al. [20,21], afterwards, developed a multiphase porous media model of deep-fat frying that can be applied to both frying and post-frying cooling to predict important industrial food quality parameters such as oil pick up and acrylamide content. The model was validated with the experimental

results of Ref. [12] and a better agreement was obtained compared with the previously developed model of Ni [15].

Datta [22] presented the relationship between various models used to study simultaneous heat and mass transfer in food processes, starting from the most elaborate multiphase porous medium model that includes evaporation and going down in complexity to the simplest equation of isothermal diffusion. A more general multiphase porous media model with distributed evaporation was shown to effectively describe a number of heat and mass transfer processes in foods in Ref. [23]. Most recently, Farid [24] presented a unified approach to food dehydration, which was based on a moving boundary [25] and previous studies [26,27] which used a single equation to describe the dehydration processes of food with different geometries. It was concluded that the developed method can account for moisture diffusion and could be used to predict heat and mass transfer in all drying and frying processes. The single parameter defined in Ref. [24] is a physical parameter, which reflects the extent of mass diffusion relative to thermal diffusion. It was dealt by using an empirical parameter due to the lack of information of physical properties of food such as moisture permeability and crust thermal conductivity.

Examination of above researches indicates that the vast majority of the published works has mainly concentrated on the investigation and modelling of the heat and mass transfer processes for a single or a batch product in the laboratory. However, batch frying is not common at the industrial scale since it is more costly than

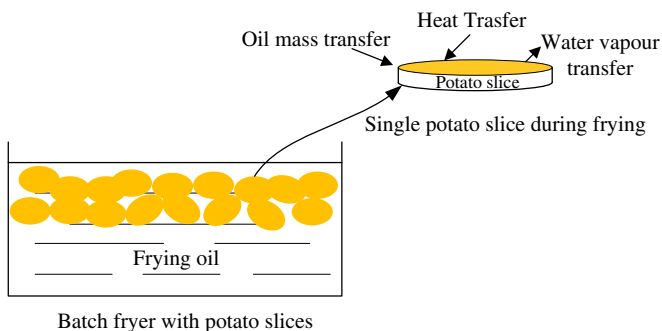


Fig. 1. A generic schematic of frying process (batch and single potato slice).

continuous frying [28]. In addition, the design and operation of industrial continuous frying processes is a relatively complex mechanism, which is still not clearly understood. To the best knowledge of the present authors, only limited work has been reported on continuous frying systems such as that reported in Refs. [29–32]. Rywotzki [29] presented an analytical model of thermal energy used during the process of food frying. It was concluded that the analysis of the energy balance in the process of food frying makes possible the formulation of a detailed mathematical model allowing calculation of the energy requirement for actual conditions. Brescia and Moreira [30], analysed the dynamics of a continuous frying process using X (exogenous input), ARX (autoregressive with exogenous input), and ARMAX (autoregressive moving averaging with exogenous input) models. They concluded that both ARX and ARMAX models could simulate the process adequately and final colour and oil content could be used as the control parameters for the process. Rywotzki [31] developed a control system for a frying process using logical, programmable controllers based on fuzzy logic. It was found that there is a possibility of increasing the frying process efficiency while maintaining the required food quality features. Nikolaou [32] developed a one-dimensional model and control for an industrial continuous snack-food frying system. However, the model did not consider the surface water of the raw material, normally between 4% and 10% by weight based on on-site measurements by the factory engineers and verified by the present authors (The data used in this study relate to a factory located in the UK). In addition, the free frying section (see Section 2, Fig. 3) and post-frying processes were also not considered. Most recently, Wu et al. [33,34] studied the energy flows in crisp frying using a First Law of Thermodynamics modelling approach in order to identify opportunities for energy conservation measures. However, the mechanism of industrial continuous frying processes, especially the fryer, is still not fully understood and there is still much need for further investigation.

In the present study, the aim is to establish a two-dimensional transient model capable of predicting temperature, moisture content and oil uptake during continuous frying processes, and to consider its applicability to the simulation of an industrial

continuous fryer system and any new phenomena pertinent. Finally, a sensitivity analysis is carried out to examine the effects of the main process variables on the final product properties. In future work, the established dynamic model can be further modified and used in the overall frying system for the purposes of design and controlling the system for assessing potential energy savings.

2. Mathematical modelling for a continuous fryer

2.1. Description of the frying system

The frying system, shown schematically in Fig. 2, consists mainly of three major components: the combustor, the oil heat exchanger and the fryer [33]. In the combustor, a gas burner burns natural gas with fresh air and foul gas (vapours from the fryer) to produce combustion gases that flow through a heat exchanger to heat up the frying oil that is re-circulated through the fryer. In many cases, exhaust gas recirculation is used to increase turbulence, provide combustor surface cooling and reduce emissions. Directing the vapours generated from the frying process from the fryer to the combustor where they are incinerated reduces not only the emissions but also the smell coming from the plant.

The actual details of the fryer is consistent with the previous study of Wu et al. [34], and will only be described briefly here for the sake of completeness. A typical commercial fryer, see Fig. 3, is around 11 m long (up to the takeout conveyor) and 30 cm deep. Before fried, the potato slices, usually 2–3 mm in thickness and 30–40 mm in diameter, are fed into the fryer by a conveyor from the dewatering system, which is designed to remove surface water (5–10% of raw potato slices by mass) from the slices. After free frying for a few seconds, the potato slices are kept submerged in oil by rotating paddles, whose rotating speed can be changed to adjust the heat transfer coefficient between frying oil and potato slices. The hold down speed will adjust the residence time of the slices in the fryer in order to control the final moisture content. This, alongside other parameters such as the mass flow rate of the raw potato slices and oil temperature, determines the final properties of the potato crisps exiting the fryer. The temperature of the

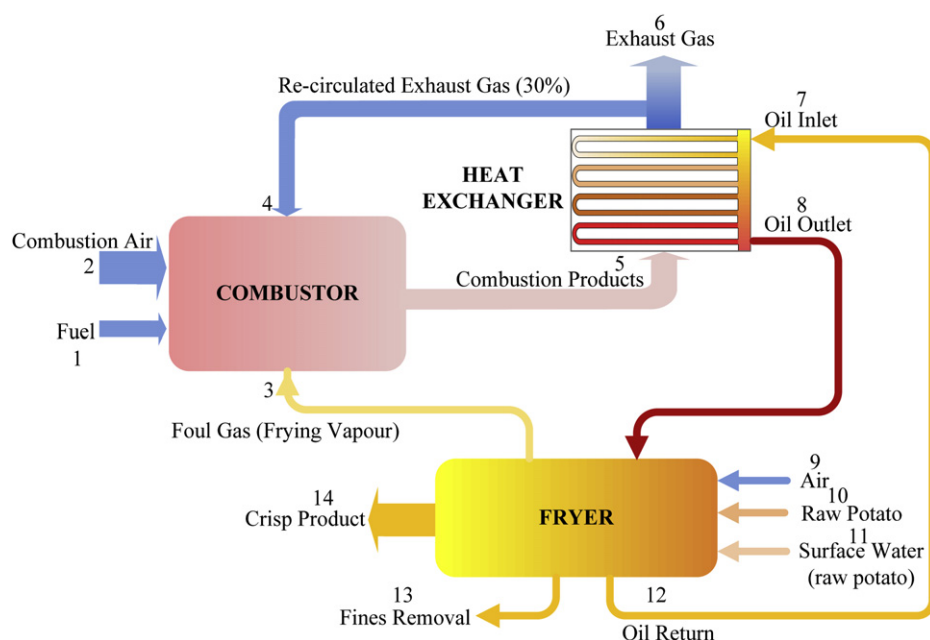


Fig. 2. Schematic diagram of frying system.

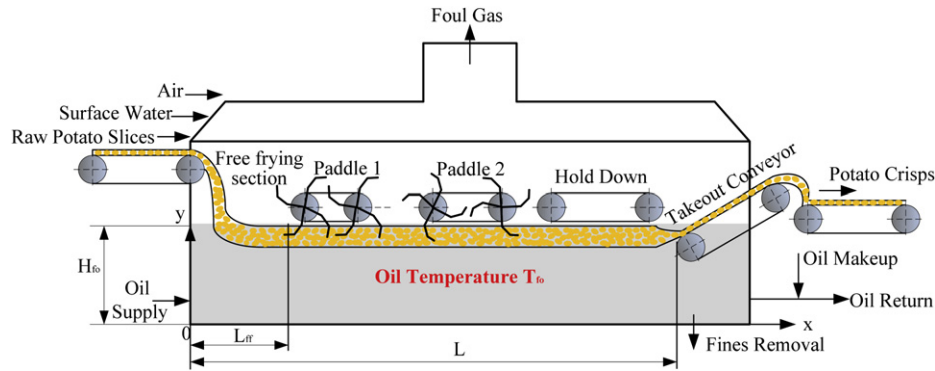


Fig. 3. Schematic flow diagram of an industrial continuous fryer.

circulating oil drops by around 20 K during frying, mainly due to the energy used to evaporate the moisture inside the potato slices. The cooler oil exiting the fryer is then passed into a heat exchanger, where the oil is reheated to the required temperature and pumped into the inlet of the fryer. The crisps leaving the fryer are allowed to cool with further oil uptake (post-frying), and then they are seasoned and transported for packaging. The temperature for the seasoning could be marginally higher than the ambient temperature. The final moisture content and oil content are controlled to be at around 1.5% (wet basis) and 35% (wet basis) with an approximate standard deviation of 0.28 and 1.6, respectively.

2.2. Major assumptions

The simplified two-dimensional physical configuration inside the fryer for the present model is illustrated in Fig. 4. Coordinates x and y denote the horizontal and vertical direction along the fryer, respectively.

The following major assumptions are made in the derivations of the governing equations:

- The potato slice is considered to be homogeneous and isotropic, and the initial moisture and temperature distribution in the potato slice are uniform;
- The potato crust is assumed to be negligible and has the same properties as the whole sample;
- Each potato slice is considered as an infinite slab, which implies that the heat and mass transfer occur only in the direction perpendicular to the slice surface;

- The heat required for chemical reaction (i.e. starch gelatinization, protein denaturation) is small compared to the heat required to evaporate the water and thus will be ignored in the present study [14,33];
- The effects of overall shrinkage during frying are neglected and the product is fried symmetrically;
- The temperature gradient after free frying section along fryer cross section is constant;
- Heat losses to the environment are negligible.

Other simplifications are described in the due course in the rest of the paper.

2.3. Governing equations

The mathematical model includes two main processes: frying process that begins when the products are dropped into the fryer and lasts until they are taken out from the fryer, and post-frying cooling process that begins when the products are removed from the hot oil and lasts until they achieve the ambient temperature. Based on the above assumptions, the set of governing equations for the frying oil, potato slice and oil uptake are as follows:

2.3.1. Frying oil

The frying oil temperature during the continuous frying process can be modelled using an energy balance within the controlled volume of the frying oil. The equation for calculating the changes in the temperature of the frying oil in vector form is:

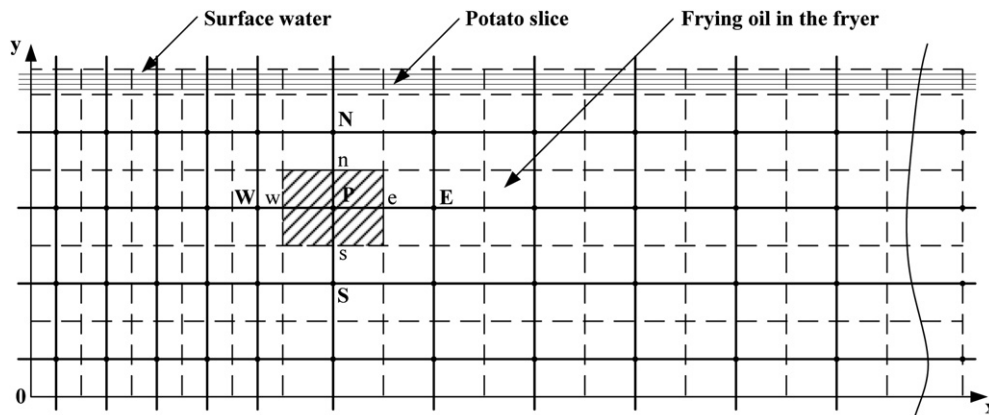


Fig. 4. Control volume mesh used for all computation (not to scale).

$$\frac{\partial(\rho_{fo}c_{pfo}T_{fo})}{\partial t} + v_{fo,x}\frac{\partial(\rho_{fo}c_{pfo}T_{fo})}{\partial x} + v_{fo,y}\frac{\partial(\rho_{fo}c_{pfo}T_{fo})}{\partial y} = \nabla \cdot (k_{fo}\nabla T_{fo}) - h_{fs}A_p(T_{fo} - T_{pss}) \quad (1)$$

Based on the fact that the oil flows only in the x direction ($v_{fo,y} = 0$), Eq. (1) can be rewritten as:

$$\frac{\partial(\rho_{fo}c_{pfo}T_{fo})}{\partial t} + v_{fo,x}\frac{\partial(\rho_{fo}c_{pfo}T_{fo})}{\partial x} = k_{fo,x}\frac{\partial^2 T_{fo}}{\partial x^2} + k_{fo,y}\frac{\partial^2 T_{fo}}{\partial y^2} - h_{fs}A_p(T_{fo} - T_{pss}) \quad (2)$$

where ρ_{fo} is the density of the frying oil, c_{pfo} is the specific heat of the frying oil. T_{fo} is the frying oil temperature, $v_{fo,x}$ and $v_{fo,y}$ are the oil flow velocities along the x and the y direction, k_{fo} is the thermal conductivity of oil, h_{fs} is the heat transfer coefficient between the oil and the potato slice surface. A_p is the specific area between the oil and potato slice surface per unit volume of oil and T_{pss} is the surface temperature of the potato slice.

2.3.2. Potato slice

The temperature change of the potato slices can be described by the energy balance equation in two dimensions:

$$\frac{\partial}{\partial t}[(\rho c_p)_{eff,ps}T_{ps}] + v_{ps,x}\frac{\partial}{\partial x}[(\rho c_p)_{eff,ps}T_{ps}] + v_{ps,y}\frac{\partial}{\partial y}[(\rho c_p)_{eff,ps}T_{ps}] = \nabla \cdot (k_{eff,ps}\nabla T_{ps}) + S_{VF_w}\rho_w h_{fg} \quad (3)$$

Assuming that the potato slice flow in the x direction only ($v_{ps,y} = 0$), Eq. (3) can be written as:

$$\frac{\partial}{\partial t}[(\rho c_p)_{eff,ps}T_{ps}] + v_{ps,x}\frac{\partial}{\partial x}[(\rho c_p)_{eff,ps}T_{ps}] = k_{eff,ps,x}\frac{\partial^2 T_{ps}}{\partial x^2} + k_{eff,ps,y}\frac{\partial^2 T_{ps}}{\partial y^2} + S_{VF_w}\rho_w h_{fg} \quad (4)$$

By volume averaging, and based on the fact that $\rho_w \gg \rho_v$ and $k_w \gg k_v$, the following equations are obtained:

$$(\rho c_p)_{eff,ps} = \rho_s c_{ps} VF_s + \rho_w c_{pw} VF_w \quad (5)$$

$$k_{eff,ps,(x|y)} = k_s VF_s + k_w VF_w + k_{fo} VF_{fo} \quad (6)$$

where ρ_{ps} , ρ_s , ρ_w , ρ_v are the density of potato slice (potato solid material plus water), potato solid (only the solid part), water and water vapour, respectively. c_{pps} , c_{ps} , c_{pw} are the specific heats of the potato slice, potato solid and water respectively, and $(\rho c_p)_{eff,ps}$ and T_{ps} are the effective heat capacity and temperature of the potato slice. $v_{ps,x}$ and $v_{ps,y}$ are the potato slice flow velocities along the x and the y direction, $k_{eff,ps}$ is the effective thermal conductivity of the potato slice, and k_s , k_w , k_{fo} are the thermal conductivity of the potato slice, water and frying oil. S_{VF_w} is the water vapour source term, h_{fg} is the latent heat of vapourization, and VF_s , VF_w and VF_{fo} are the volumetric fraction of potato slice, water and frying oil of potato slice, respectively.

2.3.3. Vapour source term

Tracking of the interface between water and vapour is accomplished by the solution of a volume fraction continuity equation (VOF model—volume of fluid model) for the water phase, i.e.

$$\frac{\partial(VF_w)}{\partial t} + v_{ps,x}\frac{\partial(VF_w)}{\partial x} + v_{ps,y}\frac{\partial(VF_w)}{\partial y} = S_{VF_w} \quad (7)$$

Taking $v_{ps,y} = 0$, Eq. (7) can be simplified as

$$\frac{\partial(VF_w)}{\partial t} + v_{ps,x}\frac{\partial(VF_w)}{\partial x} = S_{VF_w} \quad (8)$$

2.3.4. Oil uptake

The oil uptake in vector form is given below:

$$\frac{\partial(VF_{fo})}{\partial t} + v_{ps,x}\frac{\partial(VF_{fo})}{\partial x} = \nabla \cdot (D_{fo}\nabla VF_{fo}) \quad (9)$$

where D_{fo} is the apparent diffusivity of the frying oil.

Use of Eq. (9) does not require the knowledge of temperatures, i.e. solution of the energy equation. Thus, if temperatures are not of interest, Eq. (9) is used to describe oil uptake transport. The variation of the apparent diffusivity coefficient with temperature was assumed to follow an Arrhenius type relationship.

2.3.5. Foul gas temperature

To reduce emissions and smells, vapours (foul gas) generated from the frying process are directed from the fryer to the combustor where they are incinerated. The foul gas temperature is an important input in the whole frying system [34].

The energy balance between the frying oil and the air is represented by equation:

$$\dot{m}_a c_{pa}(T_{FG} - T_a) = \dot{m}_v c_{pv}(T_v - T_{FG}) + h_{fa} A_{eff}(T_{fo} - T_c) \quad (10)$$

where \dot{m}_a and T_a are the mass flow rate and temperature of air at the inlet of the fryer, c_{pa} and c_{pv} are the specific heats of air and vapour. T_{FG} is the temperature of foul gas, \dot{m}_v and T_v are the mass flow rate and temperature of the vapour produced during the frying process, h_{fa} is the heat transfer coefficient between the frying oil and air, and A_{eff} is the effective heat transfer area of air. T_c is the characteristic temperature defined by

$$T_c = (T_a + T_{FG})/2 \quad (11)$$

The foul gas temperature can be derived by substituting Eq. (11) into Eq. (10), i.e.

$$T_{FG} = \frac{\dot{m}_a c_{pa} T_a + \dot{m}_v c_{pv} T_v + h_{fa} A_{eff}(T_{fo} - T_a/2)}{\dot{m}_a c_{pa} + \dot{m}_v c_{pv} + h_{fa} A_{eff}/2} \quad (12)$$

2.3.6. Initial conditions

Assuming that the fryer is initially at steady state, the initial conditions for Eqs. (2) and (4) are

$$T_{fo}(x,y)|_{t=0} = T_{fo,ss}(x,y) \quad (13)$$

$$T_{ps}(x,y)|_{t=0} = T_{ps,ss}(x,y) \quad (14)$$

where the subscript ss denotes steady state.

The initial conditions for the velocity of oil and the potato slice are as follows:

$$v_{fo}(x,y)|_{t=0} = v_{fo,in}(x) \quad (15)$$

$$\begin{cases} v_{ps}(x, y)|_{t=0, x \leq L_{ff}} = v_{fo, in}(x, y) \\ v_{ps}(x, y)|_{t=0, L_{ff} < x \leq L} = v_{ps, ss}(x, y) \end{cases} \quad (16)$$

where L_{ff} is the length of free frying section and L is the distance along the fryer up to the takeout conveyor.

The initial conditions for Eqs. (8) and (9) are given by:

$$VF_w(x, y)|_{t=0} = VF_{w, ss}(x, y) \quad (17)$$

$$VF_{fo}(x, y)|_{t=0} = 0 \quad (18)$$

2.3.7. Boundary conditions

The boundary conditions for frying oil in the fryer is

$$\frac{\partial T_{fo}}{\partial x} \Big|_{t, y=L} = 0 \quad (19)$$

$$\frac{\partial T_{fo}}{\partial y} \Big|_{t, y=\begin{cases} 0 \\ H_{fo} \end{cases}} = 0 \quad (20)$$

At the centre of the potato slice, symmetry boundary conditions are used, i.e.

$$\frac{\partial T_{ps}}{\partial y}(t, x, 0) = 0 \quad (21)$$

$$\frac{\partial VF_{fo}}{\partial y}(t, x, 0) = 0 \quad (22)$$

The boundary conditions for the oil temperature and the potato slice temperature at the inlet of the fryer are

$$T_{fo}(t, 0, y) = T_{fo, in}(t) \quad (23)$$

$$T_{ps}(t, 0, y) = T_{ps, in}(t) \quad (24)$$

The boundary conditions for the volume fraction of the moisture content and the oil content of potato slice are

$$VF_w(t, 0, y) = VF_{w, in}(t) \quad (25)$$

$$VF_{fo}(t, 0, y) = 0 \quad (26)$$

The boundary conditions at the frying surface of the potato slice are given by:

$$k_{eff, ps} \frac{\partial T_{ps}}{\partial y} \Big|_{t, y=\frac{\delta_{ps}}{2}} = \begin{cases} h_{fs}(T_{fo} - T_{ps, ss}); & 0 < x \leq L \\ h_a(T_{amb} - T_{ps, ss}); & x > L \end{cases} \quad (27)$$

$$VF_{fo}\left(t, x, \frac{\delta_{ps}}{2}\right) = VF_{fo, surf} \quad (28)$$

where δ_{ps} is the thickness of potato slice, T_{amb} is the average ambient temperature and is assumed to be 298 K in the current analysis.

This equation is a very simple assumption for the oil boundary. In fact, the volume fraction near the surface occupied by the oil may not be a constant. It could depend on whether there is bubbling because bubbles can push out the oil from the surface. In the current study, it is assumed that the oil volume fraction on the surface is constant with a time-averaged value of 10% (wet basis) during frying and 35% (wet basis) during post-frying cooling.

Possible future availability of a more phenomenological model of surface adsorption of oil may enhance the transport model presented here.

2.4. Input parameters

The input parameters are vital in yielding an accurate predictive model. This study aims to simulate the real industrial food frying process and the effect of new design on the physical system. In the current study, the crisp frying process is used as a case study although it is reasonable not to limit the analysis to specific materials. The selected input data in the model are listed in Table 1 and they are selected from either a real continuous fryer operations in a UK factory or previously published references.

2.5. Numerical scheme

The two-dimensional computational domain inside the fryer shown in Fig. 4 was divided into a series of non-overlapping control volumes and Eqs. (2), (4), (8) and (9) were integrated within each control volume. If we take ϕ as the generalized variable for T and VF , the coupled governing equations, initial conditions and boundary equations can be discretized into a set of algebraic equations using a first order upwind scheme of the convection terms when they are included, with fully implicit finite volume scheme and variable time-steps, in the form of

$$a_P \phi_P = a_E \phi_E + a_W \phi_W + a_N \phi_N + a_S \phi_S + b \quad (29)$$

where a_P , a_E , a_W , a_N , and a_S are the coefficient matrix and b is the source term.

Since these layers are coupled together, the corresponding four sets of equations have to be solved simultaneously. This complex conjugate problem is tackled with the variable time-step finite volume method. The most attractive feature of this method is the fact that the resulting solution would imply that the integral conservation of energy is exactly satisfied over any group of control volumes and over the whole computation domain. The governing equations along with their initial and boundary conditions were solved numerically with alternating direction implicit (ADI) method programmed with Visual C++. In order to reduce the error caused by the explicit format, a sufficiently fine grid was used. During the program, test solutions for a typical operation were

Table 1
Some of the input parameters used in the computations.

Input parameters	Value or expressions	Unit	Source
c_{pfo}	2.34	kJ/kg K	Plant data
c_{ps}	1.3	kJ/kg K	Plant data
D_{fo}	$D_{fo,0} \exp \left[\frac{E_{a,fo}}{R_g T_{fo}} \right]$	m ² /s	[32]
h_{fg}	2256.7	kJ/kg	[32]
h_{fs}	250; $0 < x \leq L_{ff}$ 650; $L_{ff} < x \leq L$	W/m ² K	
H_{fo}	0.3	m	
L_{ff}	2.0	m	Assumed
L	11.0	m	Measured
\dot{m}_{tps}	1.2	kg/s	Assumed
\dot{m}_{sw}	5% $\times \dot{m}_{tps}$	kg/s	Measured
$T_{fo, in}$	446	K	Plant data
$T_{ps, in}$	333	K	Plant data
v_{fo}	0.3	m/s	Assumed
v_{ps}	0.3; $0 < x \leq L_{ff}$ 0.1; $L_{ff} < x \leq L$	m/s	Assumed
VF_{w0}	0.75	—	Plant data
δ_{ps}	2	mm	Plant data
ρ_{fo}	811	Kg/m ³	Plant data

obtained by utilizing different grid sizes to check the grid independence. It was found that 7000-grid is economic with sufficient grid independence for all subsequent simulations in the present study. At each time step, the solution is considered to have achieved convergence if the change in the moisture content (wet basis) of the potato slice between two successive time steps is less than 10^{-4} .

3. Numerical results and discussion

3.1. Fryer temperature profile

The frying oil temperature is an important parameter in frying because the oil serves as a heating medium in the process. Fig. 5 indicates the contour temperature profile in Kelvin of the frying oil inside the fryer plotted along the entire length and height of the fryer at steady state. Note that 2D is assumed, i.e. there is no temperature variation in the plane perpendicular to the length of the fryer after the free frying section. It is clearly seen that the temperature of the oil decreases significantly during the free frying section (within a 2 m distance from the fryer inlet) where the potato slice is dropped into the fryer. As frying progresses, the frying oil temperature distribution appears to be changing uniformly along the fryer. As seen in Fig. 5, after the free frying section, the temperature is fairly uniform along the height of the fryer, probably due to the mixing induced by the rotating paddles.

Although contour plots are probably a more accurate representation of the frying oil temperature distribution, it is felt that the average temperature plots, Fig. 6, exhibited here clearly and succinctly demonstrate the temperature changes inside the fryer during the frying process. The average temperature is calculated by the control volume average along the y direction. The frying

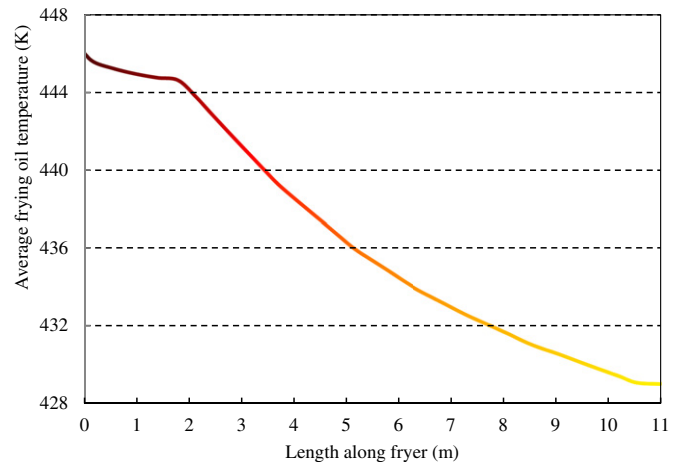


Fig. 6. Simulated average temperature of frying oil along fryer.

temperature at the exit of the fryer is about 429 K, a little higher than the temperature at the inlet of the heat exchanger (427.9 K) [34]. This implies that about 1–2 K equivalent heat losses occur while the frying oil is circulated back to the heat exchanger. It should also be noted that, meanwhile, the temperature gradient during the free frying section is low. This is because of the fact that a heat transfer coefficient of $250 \text{ W/m}^2 \text{ K}$ was used in the present simulation compared to the higher value of $650 \text{ W/m}^2 \text{ K}$ in the rest of the fryer. The values of these two heat transfer coefficients were taken from the literature [32] based on non-boiling and boiling processes and may need to be verified in subsequent research.

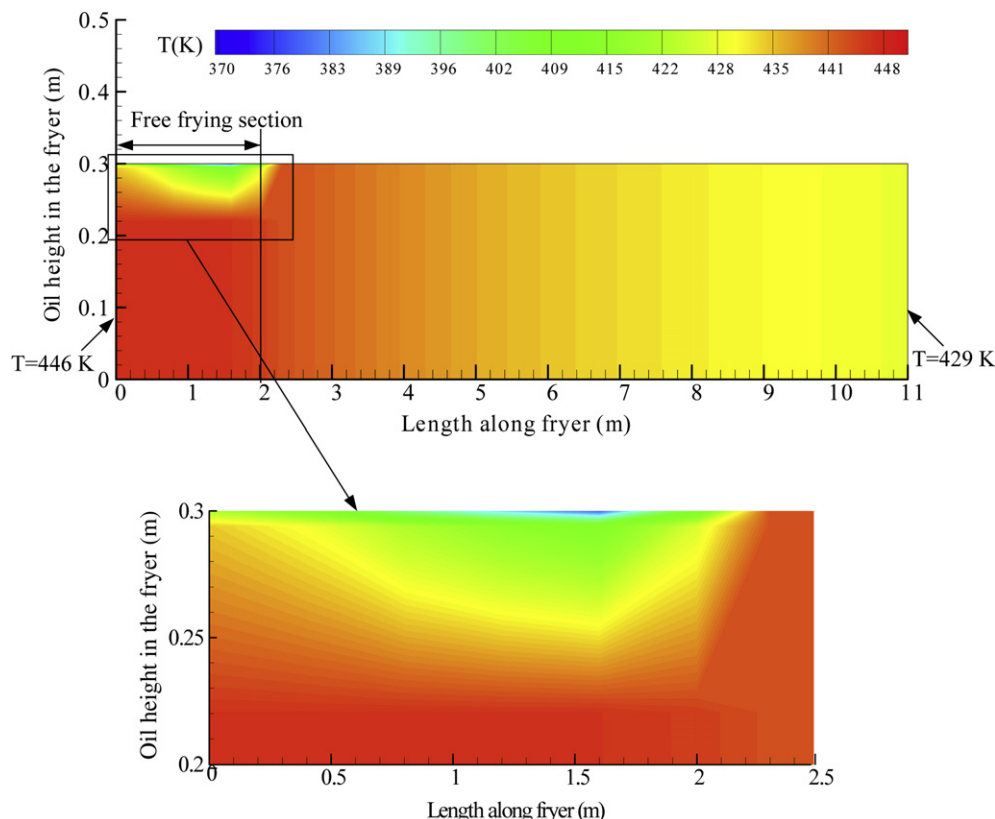


Fig. 5. Contour temperature of the frying oil inside the fryer.

3.2. Potato slice temperature

Fig. 7 shows the contour temperature plot inside the potato slice during frying. In the current study, the temperature distribution is only shown for the half thickness of the potato slice due to symmetry and based on the assumption that the potato slice in this case is completely submerged in the oil with the same magnitude of the thermal and mass transfer processes occurring on both sides. From the study, it can be seen that the potato slice warms up from its boundary to the inside for a short time. Subsequently, the slice is still warming up while the surface water starts to evaporate. Afterwards, the temperature keeps increasing more quickly due to the higher heat transfer coefficient produced by the rotating paddles, see Fig. 3. As frying progresses, the temperature difference between the surface of the potato slice and the frying oil is relatively small.

The potato slice temperature and surface water thickness calculated as control volume average along the y direction of the potato slice during frying predicted by the model is shown in Fig. 8(a). At the beginning of frying, the plot shows an initial moderate increase in the potato slice temperature to a point at the end of the free frying section. This trend is believed to be due to the fact that the heat transfer coefficient in the free frying section is small ($250 \text{ W/m}^2 \text{ K}$). A relatively high heat transfer coefficient ($650 \text{ W/m}^2 \text{ K}$) after the free frying section would lead to an accelerated frying process; this results in a sharp rise in the temperature and a fast drop in surface water. As it is expected, the temperature then remains stable for some time until all the surface water was vaporized (this is estimated to be $\sim 15 \text{ s}$ based on the current computation). Details about surface water will be discussed in the latter part of the paper. From there till the end of the frying processes the temperature increases gradually. The average temperature of the potato slice at the exit of the fryer is approximately 407 K (134°C). Once the frying period ends, the products are taken out from the fryer, the post-frying cooling begins and the temperature within the slab starts to decrease. The cooling problem can be formulated as an unsteady heat conduction process under natural convection conditions. The amount of water that evaporates during the cooling period is negligible. It can be seen from Fig. 8(b) that the average temperature of the potato slice decreases from 407 K to 298 K within 2.5 min of cooling. This is important for the model and analysis for oil absorption during post-frying cooling. It should also be noted that a significant temperature gradient exists during the early stages of cooling, which could mainly depend on the products thickness.

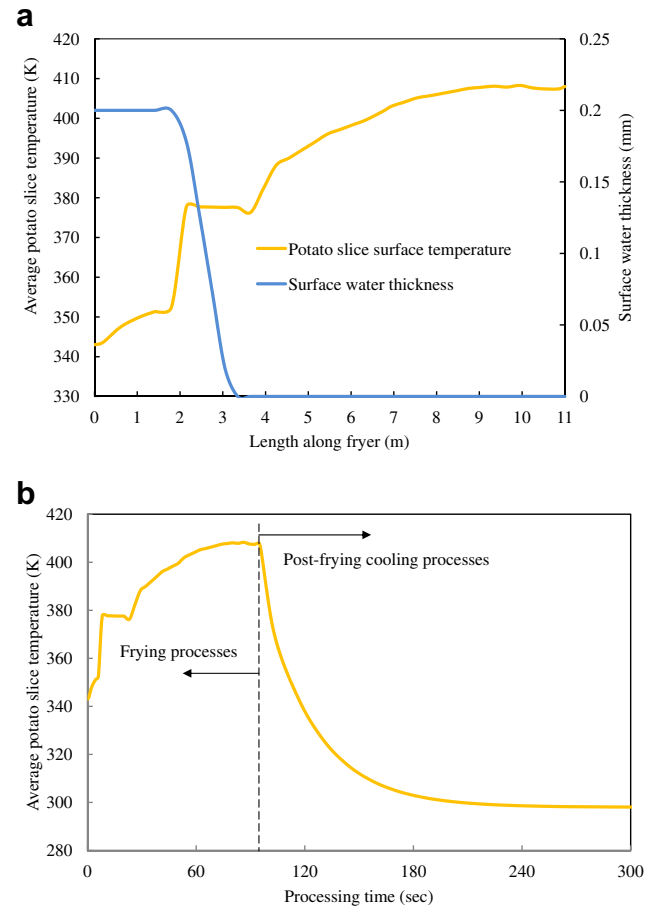


Fig. 8. (a) The variation of averaged surface temperature and surface water thickness of the potato slice along the fryer; (b) averaged temperature profile of the potato slice during frying and post-frying cooling.

3.3. Moisture content

In the frying process, moisture content and oil content distributions are important factors which determine the quality of the product. The moisture content distribution is influenced by the temperature distribution. Fig. 9 shows the computed moisture content distribution inside the potato slice. The results in Fig. 9 clearly show that surface water evaporates until there is no

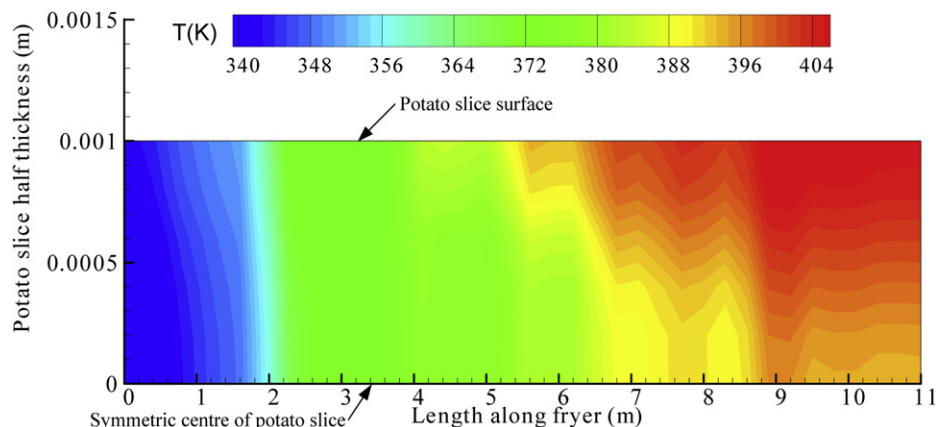


Fig. 7. Contour temperature inside the potato slice.

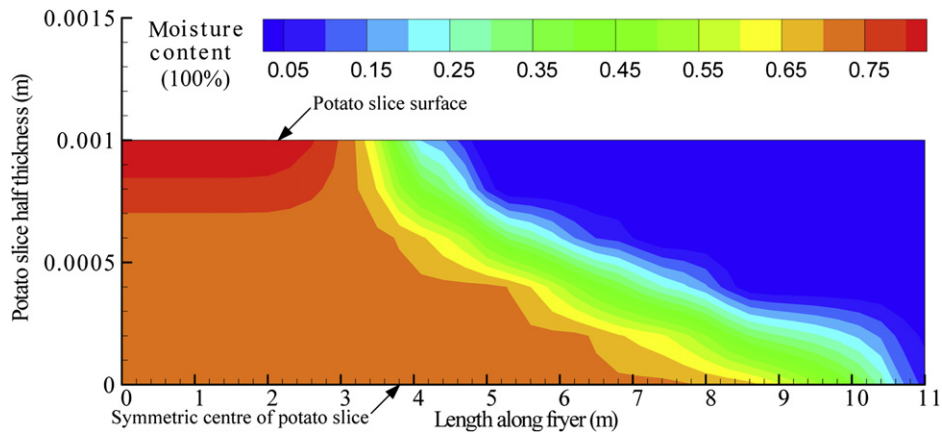


Fig. 9. Contour moisture content (wet basis) profile inside potato slices.

surface water left at nearly 3.2 m distance from the fryer inlet. This result is almost identical to the result discussed in Fig. 8. Afterwards, the moisture inside the potato slice starts to evaporate and this lasts for almost the entire length of the fryer. The moisture content is assumed to remain constant during post-frying cooling when the crisps are removed from the fryer. The computed final moisture content is approximately 1.3% by weight.

3.4. Oil content

As stated previously, the oil content of fried foods is an important quality parameter. Fig. 10 presents the contour plot of the oil absorption in percentage (wet basis) of the potato slice during the frying process. It can be observed that within the first 4 m, the oil content is almost zero. This coincides with the initial period of time at which surface water from the potato slice will evaporate.

Fig. 11 depicts the evolution of the average moisture content, oil content and surface water thickness with processing time. The total time required for complete frying is around 1.5 min (96 s) as shown in Fig. 10. In the current study, the initial thickness of surface water is 0.2 mm, which corresponding to a 5% of raw potato slices by weight. As shown in this figure, it takes about 15 s for the surface water to be removed completely. Considering energy savings, the surface water of the raw potato slices should be removed as much as possible from a practical point of view. This is consistent with the previous results obtained by Wu et al. [33].

In the real plant, it takes about eight minutes from the raw potato slices entering the fryer till the final oil uptake is measured

with a NIR (Near Infrared Reflection) gauge at the factory. It can be seen in Fig. 11 that there is a quick uptake of oil after about 15 s corresponding to the removal of surface water of the potato slice. After the initial influx, and starting from 15 s till the end of the frying process, there is a gradual absorption of oil, with the oil content at the exit of the fryer being around 7% by weight. This small amount of oil absorption is due to the flow of oil from the outside to the inside and is impeded by the vigorous outflow of vapour during frying. After the crisps are taken out of the frying oil, a higher temperature difference develops between the surface and the interior, which will generate a higher negative pressure in the pore spaces leading to significant amount of oil absorption during post-frying cooling [35]. It is noted that a rapid oil uptake is found within 2.5 min of post-frying cooling and then slows down. From the earlier observation, see Fig. 8(b), it is shown that less oil absorption occurs when the temperature of the crisps is closer to the ambient temperature. The computed final oil content of the crisps at minute 8 is 32% (wet basis), hence oil absorption that takes place during post-frying cooling contributes to nearly 78% of the total oil uptake. Future work will compare our results with the oil absorption model that was developed based on the capillary pressure driven mechanism [20,21] to further identify the main factors and conditions that affect oil absorption.

3.5. Effect of frying oil temperature

Fig. 12 shows a comparison between predicted final moisture and oil content and data obtained from the plant at different frying

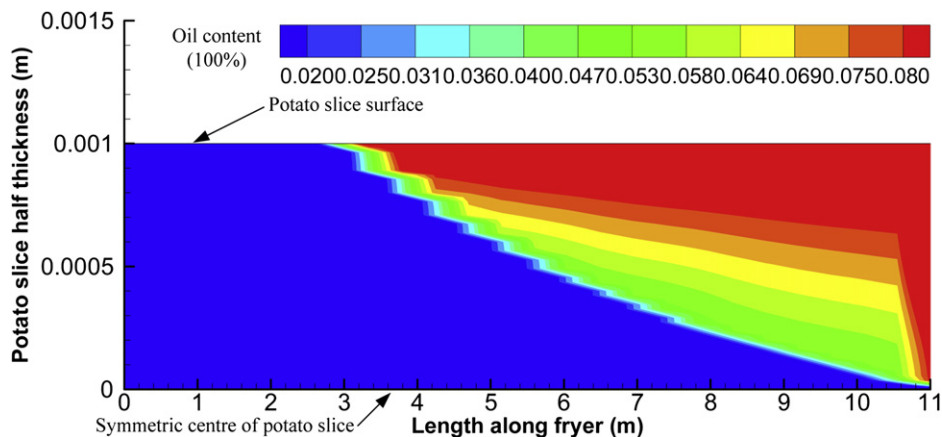


Fig. 10. Contour oil uptake (wet basis) inside the potato slices.

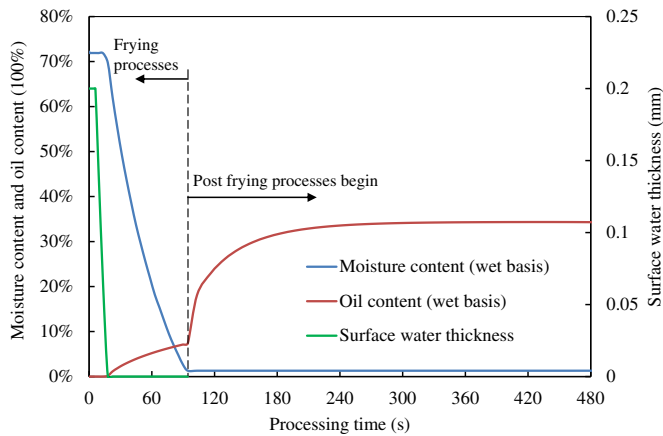


Fig. 11. Variation of average moisture content, oil content and surface water thickness with processing time.

oil temperature. Fig. 12(a) shows a ten minutes period of frying oil temperature obtained from the real plant during continuous operation of the fryer. In the current study, only some actual plant data points are compared with the simulated results since the frying oil temperature is normally in the range of 170–175 °C. The changes in oil temperature shows several fluctuations at final moisture and oil content as expected. And it is noted that there may have been a slight over-estimation or under-estimation of moisture and oil content. This could be mainly due to the fact that the current model assumes constant mass flow rate, initial constant moisture content and surface water content of the potato slices whereas in the real process there are fluctuations in the operational and control parameters. Despite this, it can be seen that in general there is a good agreement between the predicted and actual final

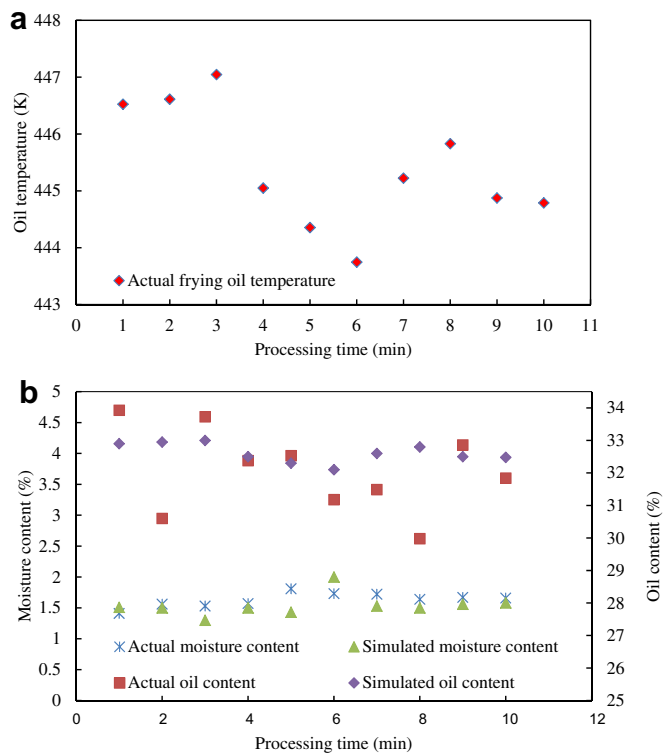


Fig. 12. Plant actual oil temperature (a) and actual and predicted final moisture and oil content (b) during continuous frying.

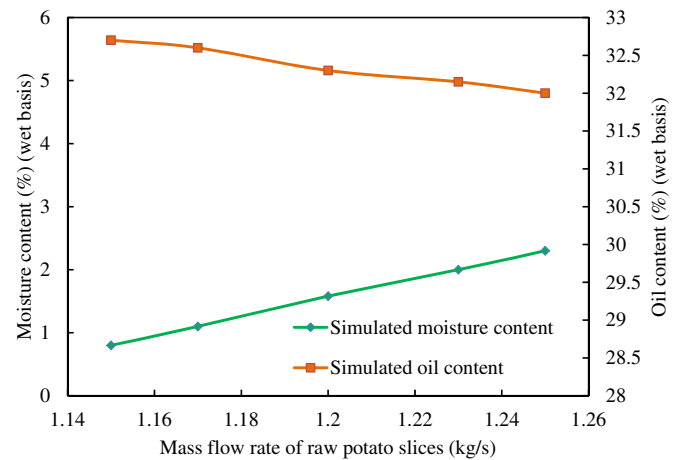


Fig. 13. Sensitivity of mass flow rate of raw potato slices to the predicted crisp final moisture content and oil content.

moisture and oil content of the crisps. This dynamic simulation also provides an insight into the sensitivity of the response of the main output parameter of the process (moisture content and oil content) to perturbations of the control (input) variables (mass flow rate and flowing speed of raw potato slices in the fryer). More detailed and carefully obtained experimental data (with a specified level of accuracy) are needed to allow researchers to proceed with a full validation of the model. In addition, some carefully controlled experiments are also needed to obtain heat transfer coefficients to be used in the modelling process.

3.6. Effect of mass flow rate of raw potato slices

One of the purposes of carrying out simulations is to seek an efficient control to fry the product to a desired moisture and oil content with acceptable variation including changes in operating conditions. It is believed that the mass flow rate of raw potato slices is an important model parameter to influence the final moisture content and oil content although experimentation to directly measure this is unavailable. Fig. 13 shows the variations of moisture and oil contents of crisps as a function of mass flow rate of the raw potato slices. Sensitivity analysis in Fig. 13 shows that, as the mass flow rate of raw potato slices is increased, less water is removed and less oil is taken. However, it is noted that the final oil content

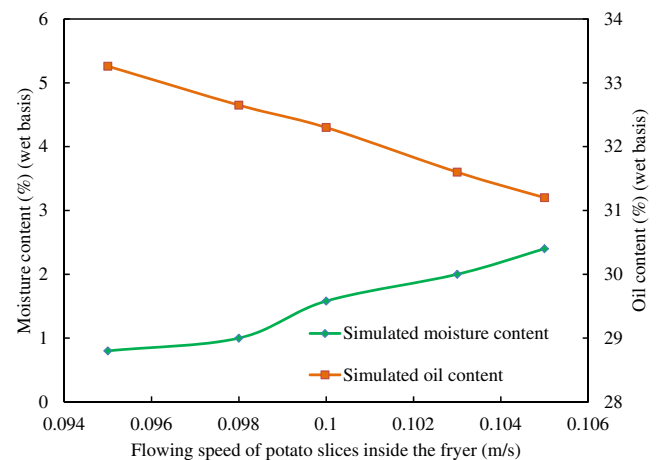


Fig. 14. Sensitivity of flowing speed of potato slices to the crisps final moisture content and oil content.

changes only by a small amount when the mass flow rate is increased from 1.15 to 1.25 kg/s.

3.7. Effect of flowing speed

Fig. 14 illustrates the effect of the flowing speed of the raw potato slices on final moisture and oil content. By increasing the flowing speed the residence time of the product in the fryer decreased. The product is exposed to the hot oil for a shorter period and, therefore, the moisture content increases as less water evaporates during frying. As a result of less cooking, less oil is taken up by the product. The curves for moisture and oil content with increasing flowing speed showed the same shape and behaviour of Fig. 13. In the real plant, to control the speed of potato slices flowing through the fryer by adjusting the rotating paddle speed accompanied with frying oil temperature is an effective way to obtain the desired final product.

4. Conclusions

A generic mathematical two-dimensional and transient model describing an industrial continuous fryer and taking into account the surface water of raw potato slices and free frying section during the frying process was developed. The proposed model is able to predict well the pattern of temperature, moisture and oil content during the continuous frying process. In general the model can be successfully applied for the design of industrial continuous frying process and for the optimization of frying conditions to obtain a better quality product and more efficient process. The developed model will be useful in the investigation of controls that can reduce energy consumption of the overall frying system.

Further validation of the model is recommended, which will require additional good quality data plus experimental analysis to confirm some of the values of the parameters used in this study such as the heat transfer coefficients.

Acknowledgements

The authors would like to acknowledge the financial support from the RCUK's Energy programme and contributions from the industrial partners and academic collaborators from the Universities of Newcastle and Northumbria. The Energy Programme is a Research Councils UK cross council initiative led by EPSRC and contributed to by ESRC, NERC, BBSRC and STFC.

References

- [1] J. Garayo, R. Moreira, Vacuum frying of potato chips, *Journal of Food Engineering* 55 (2002) 181–191.
- [2] M. Mellema, Mechanism and reduction of fat uptake in deep-fat fried foods, *Trends in Food Science and Technology* 14 (2003) 364–373.
- [3] N. Ashkenazi, Sh. Mizrahi, Z. Berk, Heat and mass transfer during frying, in: B.M. McKenna (Ed.), *Engineering in Foods*, vol. 1, Elsevier Publishers NY, USA, 1984.
- [4] M.H. Gamble, P. Rice, Effect of pre-drying of oil uptake and distribution in potato chip manufacture, *International Journal of Food Science and Technology* 22 (1987) 535–548.
- [5] M.H. Gamble, P. Rice, J.D. Selmán, Relationship between oil uptake and moisture loss during frying of potato slices from c.v. record U.K. tubers, *International Journal of Food Science and Technology* 22 (1987) 233–241.
- [6] M.H. Gamble, P. Rice, The effect of slice thickness on potato crisp yield and composition, *Journal of Food Engineering* 8 (1988) 31–46.
- [7] R. Guillamin, Kinetics of fat penetration in food, in: G. Varela, A.E. Bender, I.D. Morton (Eds.), *Frying of Food*, VCH, Chichester, England, 1988.
- [8] P. Rice, M.H. Gamble, Technical note: modelling moisture loss during potato slice frying, *International Journal of Food Science and Technology* 24 (1989) 183–187.
- [9] B.E. Farkas, Modelling Immersion Frying as a Moving Boundary Problem, Ph.D. thesis, Davis, USA, University of California, 1994.
- [10] C. Keller, F. Escher, Heat and mass transfer during deep fat frying of potato products, Poster Presented at International Congress on Engineering and Food, Cologne, Germany, 1989.
- [11] R.G. Moreira, J. Palau, X. Sun, Deep-fat frying of tortilla chips: an engineering approach, *Food Technology* 49 (1995a) 146–150.
- [12] B.E. Farkas, R.P. Singh, T.R. Rumsey, Modeling heat and mass transfer in immersion frying: model development, *Journal of Food Engineering* 29 (1996) 211–226.
- [13] B.E. Farkas, R.P. Singh, T.R. Rumsey, Modeling heat and mass transfer in immersion frying: model solution and verification, *Journal of Food Engineering* 29 (1996) 227–248.
- [14] Y. Chen, R.G. Moreira, Modeling of a batch deep-fat frying process for tortilla chips, *Transactions of IChemE, Part C: Food and Bioproducts Processing* 75 (C3) (1997) 181–190.
- [15] H. Ni, A.K. Datta, Moisture, oil and energy transport during deep-fat frying of food materials, *Transactions of IChemE, Part C: Food and Bioproducts Processing* 77 (1999) 194–204.
- [16] R. Yamsaengsung, R.G. Moreira, Modeling the transport phenomena and structural changes during deep fat frying, part I: model development, *Journal of Food Engineering* 53 (2002) 1–10.
- [17] R. Yamsaengsung, R.G. Moreira, Modeling the transport phenomena and structural changes during deep fat frying, part II: model solution & validation, *Journal of Food Engineering* 53 (2002) 11–25.
- [18] P. Bouchon, D.L. Pyle, Modelling oil absorption during post-frying cooling: I: model development, *Food and Bioproducts Processing* 83 (2005) 253–260.
- [19] P. Bouchon, D.L. Pyle, Modelling oil absorption during post-frying cooling: II: solution of the mathematical model, model testing and simulations, *Food and Bioproducts Processing* 83 (2005) 261–272.
- [20] A. Halder, A. Dhall, A.K. Datta, An improved, easily implementable, porous media based model for deep-fat frying, Part I: model development and input parameters, *Trans IChemE, Part C, Food and Bioproducts Processing* 85 (C3) (2007) 209–219.
- [21] A. Halder, A. Dhall, A.K. Datta, An improved, easily implementable, porous media based model for deep-fat frying, Part II: results, validation and sensitivity analysis, *Trans IChemE, Part C, Food and Bioproducts Processing* 85 (C3) (2007) 220–230.
- [22] A.K. Datta, Porous media approaches to studying simultaneous heat and mass transfer in food processes. I: problem formulations, *Journal of Food Engineering* 80 (2007) 80–95.
- [23] A.K. Datta, Porous media approaches to studying simultaneous heat and mass transfer in food processes. II: property data and representative results, *Journal of Food Engineering* 80 (2007) 96–110.
- [24] M.M. Farid, R. Kizilel, A new approach to the analysis of heat and mass transfer in drying and frying of food products, *Chemical Engineering and Processing* 48 (2009) 217–223.
- [25] M.M. Farid, The moving boundary problems from melting and freezing to drying and frying, *Chemical Engineering and Processing* 41 (2002) 1–10.
- [26] M.M. Farid, A unified approach to the heat and mass transfer in melting, solidification, frying and different drying processes, *Chemical Engineering Science* 56 (2001) 5419–5427.
- [27] M.C. Smith, M.M. Farid, A single correlation for the prediction of dehydration time in drying and frying of samples having different geometry and size, *Journal of Food Engineering* 63 (2004) 265–271.
- [28] R. Bou, J.A. Navas, A. Tres, R. Codony, F. Guardiola, Quality assessment of frying fats and fried snacks during continuous deep-fat frying at different large-scale producers, *Food Control* 27 (2012) 254–267.
- [29] R. Rywotycski, A model of heat energy consumption during frying of food, *Journal of Food Engineering* 59 (2003) 343–347.
- [30] L. Brescia, R.G. Moreira, Modelling and control of continuous frying processes: a simulation study. Part I: dynamic analysis and system identification, *Food and Bioproducts Processing* 75 (1997) 3–11.
- [31] R. Rywotycski, Food frying process control system, *Journal of Food Engineering* 59 (2003) 339–342.
- [32] M. Nikolaou, Control of snack food manufacturing systems, *IEEE Control Systems Magazine* 26 (2006) 40–53.
- [33] H. Wu, H. Jouhara, S.A. Tassou, T.G. Karayiannis, Modelling of energy flows in potato crisp frying processes, *Applied Energy* 89 (2012) 81–88.
- [34] H. Wu, S.A. Tassou, T.G. Karayiannis, H. Jouhara, Analysis and simulation of continuous food frying process, *Applied Thermal Engineering* (2012). <http://dx.doi.org/10.1016/j.applthermaleng.2012.04.23>.
- [35] F. Pedreschi, C. Cocio, P. Moyano, E. Troncoso, Oil distribution in potato slices during frying, *Journal of Food Engineering* 87 (2008) 200–212.